Preprints (www.preprints.org) | NOT PEER-REVIEWED | Posted: 22 January 2017 doi:10.20944/preprints201701.0096.v1

Biomineralization of Calcium and Magnesium Carbonate Minerals Induced by *Bacillus licheniformis* and Its Application in Water Softening

Short title: biomineralization induced by bacteria and application in water softening

Yanyang Zhao [1,2] and Hui Zhao [3,*]

[1] Shandong Provincial Key Laboratory of Depositional Mineralization and Sedimentary minerals, College of Earth Science and Engineering, Shandong University of Science and Technology, 266590 Qingdao, China

[2] Key Laboratory of Marine Geology and Environment, Chinese Academy of Sciences, 266071 Qingdao, China

[3] College of Chemical and Environmental Engineering, Shandong University of Science and Technology, 266590 Qingdao, China

* Correspondence: 15954804511@163.com

Abstract

Reducing the hardness of hard water is of great concern nowadays due to some adverse effects on water pipes, boilers and soap consumption. Using the method of biomineralization to precipitate calcium and magnesium ions to become carbonate minerals was one of the most important innovations for reducing the hardness of hard water. The present study sought to explore the physical and chemical conditions of carbonates bio-precipitation and the potential use of *Bacillus licheniformis* SRB2 strain (GenBank: KM884945.1) isolated from sludge sample of Moshui River (Shandong University of Science and Technology, Qingdao, China) in reducing the hardness of hard waters by the induction of carbonate minerals. In this study, *B. licheniformis* SRB2 strain was identified based on the morphological, biochemical and 16*S* rDNA gene sequence homology analysis. The carbonate minerals induced by *B. licheniformis* bacteria in the liquid culture medium with 3% NaCl and Mg/Ca molar ratio of 0, 6, 8, 10 and 12 were investigated. The culture medium was inoculated with the bacterial liquid seed was set as the experimental group and the other culture medium was inoculated with the same volume of distilled water was set as the control group. The mineral phases, micromorphologies, and crystal structures were analyzed using X-ray powder diffraction, scanning electron microscope, energy dispersive X-ray detector, high resolution transmission electron

Preprints (www.preprints.org) | NOT PEER-REVIEWED | Posted: 22 January 2017 doi:10.20944/preprints201701.0096.v1

microscopy and selected area electron diffraction. The bacterial concentrations and pH values of the solution were measured by a spectrophotometer and a pH meter, respectively. The urease secreted by *B. licheniformis* SRB2 was found to greatly increase the pH values of the liquid medium, which favored the formation of calcium carbonate.As a result, Mg^{2+} and Ca^{2+} ion concentrations decreased greatly due to the biomineralization of calcium carbonate and nesquehonite minerals in the presence of *B. licheniformis* SRB2 bacterium. There were only few calcium carbonates and no nesquehonite minerals in the control groups. It was also found that the minerals of nesquehonite induced by *B. licheniformis* SRB2 had a phenomenon of preferred orientation. What was more, even though Mg^{2+} ions inhibited the precipitation of Ca^{2+} ions, but under the action of *B. licheniformis* SRB2 bacteria, the inhibition effect was significantly declined. The bio-precipitation of calcium carbonate and nesquehonite minerals may represent a new method of pretreatment for the hardness reduction of hard water. The accomplished study is of certain interest for interpretation of the carbonates biomineralization in natural environment, and maybe also has a certain application value in the former processing of hard water

Keywords: biomineralization; calcium ions; magnesium ions; *Bacillus lichemiformis*; carbonates

1. Introduction

It has been estimated that the supply of potable water will fall by a third in 20 years [1], which leads to an increase in the demand for potable water around the world. Water softening has been an important way to produce potable water especially for some regions where potable water is lacking while seawater is easy to get [2]. The mechanism for water softening is aimed to that “chemical salt” can be removed through all kinds of physical and chemical methods. That is to say, many kinds of ions such as Mg^{2+} and Ca^{2+} ions in hard water can be removed. The current deep treatment technology for drinking water has made considerable progress and is gradually becoming widely used. But current water treatment needs to consume large amounts of energy and cost [3]. There are many kinds of production methods for water softening such as heat and membrane technologies. Thermal technology is used to remove Mg^{2+} and Ca^{2+} ions from seawater or hard water by evaporating moisture with the aid of external heat. Multi-effect distillation,

Preprints (www.preprints.org) | NOT PEER-REVIEWED | Posted: 22 January 2017 doi:10.20944/preprints201701.0096.v1

multi-stage flash and steam condensation have been considered as ordinary thermal methods [4]. Membrane technologies driven by electrical energy include reverse osmosis, membrane distillation and electroosmosis [5, 6]. However, owing to their secondary intermediates formation in these removal or treatment technologies, the inherent drawbacks have been found, what's more, the cost used for water treatment is also too high [7]. Thus, there have been many improvements in the water softening process especially in the recent decade years. Some water treatment systems have been greatly improved and changed more reliably, which now enable us to save a certain amount of funds. However, the huge consumption of energy used for water softening is still a defect and leads to high operating costs and water price. Owing to the shortage of large amounts of energy and the high costs of general softening process, there is an urgent need for a new water softening method, which is vastly cheaper and friendly to the environment. One of the new innovations in this regard is that bacterially induced biomineralization can be used to precipitate Mg^{2+} and Ca^{2+} ions for the decrease of hardness. Biomineralization treatment technology has proved to be a favorable alternative due to the fact that no toxic end products can be produced and it is more cost-effective [7].

Different species of microorganisms have different capacities of biomineralization for certain metal ions. A metal-resistant *Aeruginosa* strain has shown certain U resistance and its biomineralization capacity has reached to a maximum efficiency after incubation for 6 hours in the medium (100 mg U L^{-1}, pH 4.0) [8]. Arsenic mobility has significantly decreased in the exchangeable fraction of soil as tolerant bacterium *ginsengisoli* CR5 is present [9]. *Bacillus thuringiensis* bacterium not only has strong resistance to many kinds of metals but also has strong ability to precipitate heavy metal ions in the meanwhile [10]. The adsorbent WJ-I, harvested after the precipitation of fermentation liquid of sp. GX4-1 bacteria by alcohol, can precipitate Cd^{2+} ions in the aqueous solution [11]. Cd^{2+} ions can also be adsorbed by *Spirulina maxima* and the maximum biomineralization capacity was 43.63 mg Cd g^{-1} active cells and 37.00 mg Cd g^{-1} dry cells [12]. The thallus of *Cerevisiae* in the brewery can adsorb K^+, Na^+, Ca^{2+}, Mg^{2+} ions and so on [13]. The precipitation rate of Pb^{2+} and Cd^{2+} by *Sojae* is 69.76% and 72.28%, respectively [14]. The precipitation rate of Pb by *Aspergillus ficuum* can reach to 92.44% [15]. *Aspergillus niger* has higher adsorptive selectivity for ^{241}Am and its adsorption rate can reach to 96% [16]. In the process of gold ore wastewater treatment, Au^+,

Preprints (www.preprints.org) | NOT PEER-REVIEWED | Posted: 22 January 2017 doi:10.20944/preprints201701.0096.v1

Ag^{+}, Cu^{2+}, Fe^{3+}, Zn^{2+} ions can be precipitated on the surface of bacteria [17]. *Aspergillus ficuum* can remove uranium (U, IV) quickly from the aqueous solution and the maximum adsorption capacity is 423 mg g^{-1} (biological dry weight) [18]. Therefore, microorganisms can be used to the sewage clarification through certain metal ions precipitation.

Bacteria belonging to the genus *Bacillus* also have strong capacity for metal ions precipitation [19, 20]. The precipitation of Pb (II) by *Bacillus cereus* 12-2 isolated from lead-zinc mine tailings has been investigated and proved that the maximum capacity of Pb immobilization is 340 mg g^{-1} at pH 3.0 [21]. It has been found that *Bacillus* sp. KK1 can significantly reduce the exchangeable Pb fraction and increase Pb carbonate fraction in the selective soil with inoculation of *Bacillus* sp. KK1 bacteria in mine tailings [22]. Calcium precipitation mediated by *Bacillus megaterium* bacterium separated from a loess profile in China has been studied and shown that calcite is the dominant mineral phase when the bacteria are present [23]. The mechanism of uranium transformation from U (VI) into nano-uramphite by two indigenous *Bacillus thuringiensis* strains has been investigated and proven that these bacteria isolated from uranium mine possess a high ability of U (VI) precipitation and the maximum capacity is around 400 mg U g^{-1} biomass (dry weight) [24]. From the above we can see that what precipitated by bacillus are always heavy metals and radioactive nuclear elements and the used bacteria are rarely *B. licheniformis*, a kind of probiotics. According to the above microbiological method, if Ca^{2+} and Mg^{2+} ions in hard water can be precipitated to form mineral crystals under the effect of *B. licheniformis* bacteria, the concentration of Ca^{2+} and Mg^{2+} ions will decrease, and the purpose of water softening could be achieved. Water softening by using *B. licheniformis* bacteria is a kind of new method that is friendly to the environment and valuable for popularized application and prospect.

In this study, a bacterial strain *B. licheniformis* SRB2 was isolated and identified, and then was cultured in aqueous systems at 3% NaCl and different Mg/Ca molar ratios to induce the precipitation of Ca^{2+} and Mg^{2+} ions by biomineralization. It has been found that a large number of calcite, vaterite, monohydrocalcite and nesquehonite crystals are precipitated in the experimental group with inoculation of SRB2 bacteria, and the bio-precipitated nesquehonite has a phenomenon of preferred orientation, only few calcite and

Preprints (www.preprints.org) | NOT PEER-REVIEWED | Posted: 22 January 2017 doi:10.20944/preprints201701.0096.v1

monohydrocalcite, no nesquehonite, are crystallized in the control group without SRB2 bacteria. It has also been found that the existence of Mg^{2+} inhibits the precipitation of Ca^{2+} ions. But this inhibition effect decreased significantly under the effect of SRB2 bacteria. Therefore, this research may provide certain reference for understanding the mechanism of biomineralization used for water softening or the recycling of magnesium and calcium from wastewater. Applying SBR2 bacteria to soften hard water or recycle Ca^{2+} and Mg^{2+} ions from wastewater is very friendly to the environment, which may have certain practical application values.

2. Materials and methods

Separation and purification of the bacterial strain *B. licheniformis* SRB2

Sludge sample was collected from Moshui River in Shandong University of Science and Technology (Qingdao, Shandong, China). The collected sludge sample was processed as follows. Firstly, 10 g of the sludge sample was dissolved in 100 mL of sterile distilled water in shake flask at 37 ºC and 200 rpm for 10 min. Secondly, after the precipitation of larger particles, approximately 1 mL of sludge suspension was transferred into the enrichment medium for the isolation of bacteria (unit g L^{-1}: K_2HPO_4 0.5, NH_4Cl 1.0, $CaCl_2$ 0.1, $MgSO_4 \cdot 7H_2O$ 2.0, yeast extract 1.0, Na_2SO_4 0.5, $Fe(NH_4)_2(SO_4)_2$ 0.5, ascorbic acid 0.5, L - Cys 0.5, 60% sodium lactate solution 6 mL, distilled water 1000 mL, pH 7.2). Fe^{2+} ion can react with S^{2-} ion to generate black ferrous sulfide in the solution, indicating that the experiment has succeeded in the enrichment of sulfate-reducing bacteria (SRB). Thirdly, the supernatant was diluted 10 times with distilled water, and then the dilution was evenly daubed onto the solid medium surface to further purify SRB (unit g L^{-1}: yeast extract 3, KCl 0.25, $Fe(NH_4)_2(SO_4)_2$ 0.5, agar 20, distilled water 1000 mL, pH 7.2). All cultures were incubated in an anaerobic incubator (YQX-II, Shanghai Yuejin Medical Instrument Co., Ltd, Shanghai, China) at 37 ºC. Finally, a single colony was selected to purify by repetitive streaking onto the solid medium at least twice. A strain named *B. licheniformis* SRB2 was screened out and used to induce the mineral precipitation in this study.

Preprints (www.preprints.org) | NOT PEER-REVIEWED | Posted: 22 January 2017 doi:10.20944/preprints201701.0096.v1

Molecular identification of *B. licheniformis* SRB2 bacteria

Reagents used in this study such as lysozyme and Taq DNA polymerase were purchased from Shanghai Sangon Biotech Co., Ltd, Shanghai, China. The method adopted to extract DNA of SRB2 bacteria, polymerase chain reaction (PCR) primers, reaction system and amplification procedures were all determined according to the published articles [25]. PCR products were sequenced by Shanghai Sangon Biotech Co., Ltd, Shanghai, China. These sequences were assembled with DNAMAN 8 software, and compared with those of GenBank database. Clustal X was used for multiple sequence alignment and adjacency method was used to build the evolutionary tree of SRB2.

Preparation of liquid seed

A colony was picked and inoculated into 100 mL of sterile liquid medium (unit g L^{-1}: beef extract 5, tryptone 10, NaCl 5, pH 7.2), and then incubated at 37 ºC and 130 rpm for one day in an oscillation incubator (HZQ-F160, Harbin electronic technology development co., LTD, Harbin, China). The growth absorbance (OD_{600nm}) was measured using spectrophotometry (722s, Shanghai analysis instrument factory, Shanghai, China). The OD_{600nm}value of liquid seed was approximately 0.95.

The determination of *B. licheniformis* SRB2 bacterial urease activity

In order to determinate the urease activity of *B. licheniformis* SRB2 bacteria, *B. licheniformis* SRB2 bacteria were cultured in tubes with urea agar medium (UAM) modified from Christensen's (unit g L^{-1}: urea 20, peptone 1, sodium chloride 5, potassium dihydrogen phosphate 2, agar 20, glucose 1 and phenol red 0.012; pH 6.5). Bacterial strain were streaked on the surface of the medium and incubated at 37 °C for about six days (maximal limit of chemical hydrolysis of urea). It was found that the color of the medium was changeg from yellow to pink, indicating that the isolated bacteria have strong urease activity.

The growth curve and pH changes at different salt concentrations

2 mL of *B. licheniformis* SRB2 liquid seed was inoculated into 200 mL of liquid culture medium (unit g L^{-1}:

beef extract 5, tryptone 10, pH 7.2) with 0, 1%, 2%, 3% and 4% of sodium chloride (NaCl), which were set as the experimental groups. The other groups inoculated of the same volume of the sterile distilled water were set as the control groups. There were three parallels for both the experimental groups and the control groups. These two groups were cultured at 37 ºC and 130 rpm in the constant temperature oscillation incubator. The concentration of bacterial suspension was measured using the spectrophotometer at the wavelength of 600 nm after 0, 3, 6, 9, 12, 14, 23, 29, 35, 48 and 60 h, respectively. The pH values of bacterial suspension were measured using a pH meter (PHS-3C, Shanghai Shengke Instrument Equipment Co., Ltd, Shanghai, China).

Carbonates minerals induced by *B. licheniformis* SRB2 at different Mg/Ca molar ratios

The liquid medium (unit g L^{-1}: beef extract 5, tryptone 10, NaCl 30) with 0.01 mol L^{-1} Ca^{2+} was divided into five portions. Mg/Ca molar ratio of each portion was 0, 6, 8, 10 and 12 respectively. 10.6 g of Na_2CO_3 and 9.0 g of $NaHCO_3$ was dissolved in 100 mL of sterile distilled water and filtrated by filter membrane with a pore diameter of 0.22 μm. 3 mL of sterile Na_2CO_3 solution and 5 mL of sterile $NaHCO_3$ solution was added into 200 mL of the liquid medium at each kind of Mg/Ca molar ratio and the pH value of the medium was adjusted to 7.2 with sterile HCl and NaOH solution (1 mol L^{-1}). *B. licheniformis* SRB2 liquid seed was inoculated into the above medium with 1 % of inoculation ratio. The medium inoculated with *B. licheniformis* SRB2 was set as the experimental group, and the medium inoculated with the same volume of sterile distilled water was set as the control group. The experimental group and the control group were incubated at 37 ºC and 130 rpm in a constant temperature oscillation incubator.

The changes of Ca^{2+} and Mg^{2+} concentration

1.5 mL of the liquid in the experimental group and the control group was taken out and added into a 1.5-mL centrifuge tube respectively, and then centrifugated at 10, 000 rpm for 5 min. The supernatant was diluted 10 times with distilled water and filtrated by filter membrane with a 0.22 μm pore size. Ca^{2+} and Mg^{2+} concentrations in the filtrate were measured by atomic absorption spectrophotometer (AAS, TAS-986,

Preprints (www.preprints.org) | NOT PEER-REVIEWED | Posted: 22 January 2017 doi:10.20944/preprints201701.0096.v1

Zhengzhou Nanbei Instrument Equipment Co., Ltd., China).

Characterization of the mineral precipitates

The mineral precipitates were taken out from the medium and washed with distilled water for three times, dried at room temperature. Some precipitates were observed with scanning electron microscopy (SEM, Hitachi S-4800, Japan Hitachi Company, Japan) and elemental composition of the precipitates was analyzed with energy dispersive spectrometer (EDS, EX-450, Japan Horiba, Japan). Some precipitates were grinded sufficiently with an agate mortar and the powder was analyzed by high-resolution transmission electron microscopy (HRTEM, JEM-2100, Japan Electronics Company, JEOL, Japan) and selected area electron diffraction (SAED) to confirm the mineral phase. The analysis of interplanar crystal spacing (d) of the mineral crystals was carried out with the Digital Micrograph 3.7 software. Some other precipitates were analyzed by X-ray diffraction (XRD, D/Max-RC, Rigaku Corporation, Japan) instrument, at a 2θ angle range of 10º - 90º, with a step size of 0.02 and a count time of 8 º/ min.

3. Results and Discussion

Morphology and 16*S* rDNA identification of *B. licheniformis* SRB2

The single colonies of *B. licheniformis* SRB2 bacteria incubated at 37 ºC had a diameter of 3.0 - 5.0 mm and rough surfaces after three days of culture on the surface of solid medium without iron ions. *B. licheniformis* SRB2 bacteria were proved to be gram-positive. Fig. 1a shows *B. licheniformis* SRB2 bacterium is rod-shaped, with a length of about 1.6 μm and a width of about 0.6 μm. The full length sequence of 16S rDNA of *B. licheniformis* SRB2 has been determined as 1483 bp. The comparison of nucleotide sequence homology was conducted with the BLAST program. 15 strains with highly homologous 16S rDNA sequences and other strains belonging to the genus *Bacillus* and two strains belonging to the similar genus were selected for comparison with that of SRB2 strain. The phylogenetic tree shown in Fig. 1b was constructed with the Clustal X2 and MEGA 6 software using the neighbor-joining method. The nucleotide

Preprints (www.preprints.org) | NOT PEER-REVIEWED | Posted: 22 January 2017 doi:10.20944/preprints201701.0096.v1

sequence homology was above 97% by comparing with 16S rDNA sequences of many strains belonging to the genus *B. licheniformis* in GenBank. The SRB2 strain was most closely related to *B. licheniformis* on the phylogenetic tree based on 16S rDNA sequences, which was consistent with the physiological and biochemical characteristics of the isolated strain. Thus, strain SRB2 was identified as *B. licheniformis*.

The growth curves of *B. licheniformis* SRB2 bacteria and pH variation tendency at different NaCl concentrations

Figure 2a shows that *B. licheniformis* SRB2 bacteria at 4% NaCl concentration have begun to enter a stable phase after continuous cultivation for 14 hours, but at the same time *B. licheniformis* SRB2 bacteria at other NaCl concentrations are still at the logarithmic growth stage. Therefore, higher NaCl concentration could inhibit the proliferation of *B. licheniformis* SRB2 bacteria. Figure 2a also shows that there is no inhibition effect on the growth of *B. licheniformis* SRB2 bacteria at 3% NaCl. By this token, *B. licheniformis* SRB2 bacteria might also be used to precipitate Ca^{2+} and Mg^{2+} in the seawater, with similar NaCl concentration. Figure 2b shows that pH rises slowly at the beginning, declines after 6 h, and rises sharply at last from 7.2 to 8.2 or so. By and large, the pH variation tendency was the same as each other at different NaCl concentrations.

There was a close relationship between the pH changes of bacterial suspension and the physiological and biochemical activities of *B. licheniformis* SRB2 bacteria in this experiment. The change trends of pH (Figure 2b) were divided into three parts, namely 0 to 6h, 6 to 12h and the time beyond 12h respectively, correlating with the three phases of *B. licheniformis* SRB2 bacterial growth, namely the lag, logarithmic and stationary phase. However, the pH value declined sharply in the time range of 6 to 12h, during which time the concentration of *B. licheniformis* SRB2 bacteria reached to a maximum (Figure 2a). Thus, there existed a close relationship between the sharp decline of pH and the concentration of *B. licheniformis* SRB2 bacteria. It was also found that *B. licheniformis* WX-02 bacteria generate a large number of organic acids such as formic acid, pyruvic acid, acetic acid, lactic acid and so on, whose yield reaches its highest point at the 12th hour and then declines [26]. SRB2 bacteria belonging to the same taxonomic genus *B. licheniformis* had

similar metabolic pathways. Therefore, the sharp decline of pH was connected with the large number of organic acids generated by *B. licheniformis* SRB2 bacteria in the time range of 6 to 12 hours. The concentration of *B. licheniformis* SRB2 bacteria reached to a maximum after 12h of culture, during which time a large number of organic compounds such as trypsin and yeast extract powder were degraded by *B. licheniformis* SRB2 bacteria to release a large amount of urea, which can be degraded by urease to release ammonia. *B. licheniformis* SRB2 bacteria could secret urease, which has been determined by urease activity experiment. Ammonia was also produced through *B. licheniformis* SRB2 bacterial physiological and biochemical reactions such as transamination and deamination action of amino acids. The released ammonia could lead to a sharp rise of pH in the culture medium. The concentration of *B. licheniformis* SRB2 bacteria was lower in lag phase from 0 to 6h, during which time the pH value slightly increased. It was found that the yield of organic acids such as formic acid, pyruvic acid, acetic acid and lactic acid produced by *B. licheniformis* WX-02 strain was 0 from 0 to 6h [26]. *B. licheniformis* SRB2 may be the same as *B. licheniformis* WX-02, not producing acids during this period. The slight increase in pH value might be due to the fact that there was a small amount of residual ammonia in *B. licheniformis* SRB2 bacterial liquid seed.

In conclusion, physiological and biochemical activities of *B. licheniformis* SRB2 bacteria could result in an increase of pH. Ca^{2+} and Mg^{2+} were precipitated to form carbonate minerals induced by *B. licheniformis* SRB2 bacteria, which was closely related to the higher pH. If *B. licheniformis* SRB2 bacteria could be used in the process of water softening, a major expenditure of money, time and man power would be saved within today's context of scarce resources. Using biomineralization method to soften hard water was also friendly to the natural environment, which maybe had a certain application value.

The changes of Ca^{2+} and Mg^{2+} concentration at different Mg/Ca molar ratios

Figure 3 shows that Ca^{2+} concentration in the experimental group is significantly lower than that in the control group, indicating that *B. licheniformis* SRB2 bacteria had a strong ability to promote Ca^{2+} precipitation. It can also be seen from Figure 3 that Ca^{2+} concentration increases gradually with an increase of Mg/Ca molar ratio in both of the two groups. However, the initial Ca^{2+} concentrations in all the groups

Preprints (www.preprints.org) | NOT PEER-REVIEWED | Posted: 22 January 2017 doi:10.20944/preprints201701.0096.v1

were 0.01 M. Thus, the quantity of Ca^{2+} used to precipitate to form calcium carbonate decreased as Mg/Ca molar ratio increased. Therefore, high concentration of Mg^{2+} ion hindered the precipitation of Ca^{2+} ions. However, Ca^{2+} ion concentrations in the experimental group were far lower than those in the control group, which just illustrated that *B. licheniformis* SRB2 bacteria had an ability to decrease the inhibition effect of Mg^{2+} on Ca^{2+} precipitation. Figure 4 shows that Mg^{2+} concentration in the experimental group is significantly lower than that in the control group, indicating that SRB2 bacteria also had an ability to promote the precipitation of Mg^{2+} ion.

It has been reported that the nucleation and crystal growth of calcium carbonate can be intensely influenced by Mg^{2+} [27]. Many studies have also indicated that the existence of Mg^{2+} inhibits the rate of calcite precipitation [28-32]. Therefore, Ca^{2+} concentration in the culture medium was higher in the presence of Mg^{2+} ions in the experimental and control group, which was due to the inhibition effect of Mg^{2+} ions on calcite precipitation. Ca^{2+} concentration at each kind of Mg/Ca molar ratio in the experimental group was lower than that in the control group, indicating that *B. licheniformis* SRB2 bacteria had an excellent capability to reduce the inhibition effect of Mg^{2+} on Ca^{2+} precipitation. This kind of role from *B. licheniformis* SRB2 bacteria had more extensive application in water treatment. When Mg^{2+} and Ca^{2+} ions were present at the same time, Ca^{2+} precipitation became rather difficult due to the inhibitory effect of Mg^{2+} in hard water. The existence of *B. licheniformis* SRB2 bacteria offered a new way to solve the above mentioned problem. It has been rarely reported about making use of the microorganisms to reduce the inhibitory effect of Mg^{2+} and increase the amount of Ca^{2+} precipitation.

SEM and EDS analysis of the mineral precipitates at different Mg/Ca molar ratios

Figure 5a shows that there are a large number of uniform dumbbell-shaped mineral precipitates and a small number of spherical mineral precipitates induced by *B. licheniformis* SRB2 bacteria at Mg/Ca molar ratio of 0. The diameter of the spherical mineral precipitate is about 16 μm, almost equal to the length of dumbbell-shaped mineral precipitate. Some rod-shaped mineral precipitates similar to *B. licheniformis* SRB2 bacteria are consisting of countless nano-scale granular minerals, which are born on the surface of the

Preprints (www.preprints.org) | NOT PEER-REVIEWED | Posted: 22 January 2017 doi:10.20944/preprints201701.0096.v1

dumbbell-shaped and spherical mineral precipitates and becoming a part of the mineral precipitates, and other rod-shaped mineral precipitates pile together at random. It has been already verified that the extracellular polymeric substances (EPS) secreted by microorganisms can serve as the nucleation sites of carbonate crystals [33]. Therefore, there were a large number of microcrystalline calcite precipitated on the EPS after the adsorption of calcium ions and carbonate ions [34]. The microcrystalline calcite gradually grew up and were piled together to form the carbonate mineral shell, in which there was a *B. licheniformis* SRB2 bacterium. The mineralization process, driven by the nucleation process on the EPS with thermodynamic properties as well as chemical properties, can make the microorganism itself being encased by a carbonate layer [35, 36]. In this study, *B. licheniformis* SRB2 bacteria were encased by the rod shaped calcite shells formed by the precipitation of microcrystalline calcite in the absence of Mg^{2+}. The inner diameter of the fractured calcite shell was approximately 0.5 μm, consistent with the width of a *B. licheniformis* SRB2 bacterium. The above result illustrated that no self-protection mechanism was present for *B. licheniformis* SRB2 bacteria. The decrease of nucleation energy caused by the functional groups on the bacterial surface can induce the mineralization process more easily [37]. However, the lack of nutrition could easily lead to the death of *B. licheniformis* SRB2 bacteria encased by the dense calcite shells.

Figure 5b shows that there are many peanut-shaped mineral precipitates with a length of about 30 μm at Mg/Ca molar ratio of 6, consisting of numerous flaky minerals, no longer nano-scale granular minerals, significantly different from the dumbbell-shaped mineral precipitates in Figure 5a. There are also a small number of spherical mineral precipitates. At the same time, a large number of rod-shaped active *B. licheniformis* SRB2 bacteria appear, which were rarely seen at Mg/Ca molar ratio of 0. The common rod-shaped calcite shell of *B. licheniformis* SRB2 at Mg/Ca molar ratio of 0 were seldom seen any more at Mg/Ca molar ratio of 6. The calcite shells of *B. licheniformis* SRB2 bacteria have disappeared due to the presence of Mg^{2+}. It has been reported that Mg^{2+} can inhibit the crystallization of calcite, which is due to the fact that the stretch of single molecule on the crystal surface is hindered by Mg^{2+} adsorption on the surface of calcite [38]. The disappeared calcite shell of *B. licheniformis* SRB2 bacteria was due to the inhibition effect of Mg^{2+} mentioned above.

Preprints (www.preprints.org) | NOT PEER-REVIEWED | Posted: 22 January 2017 doi:10.20944/preprints201701.0096.v1

There are also a small number of irregular minerals in Figure 5b, formed maybe due to the aggregation of many flaky minerals. Figure 5c shows that the mineral precipitates are rod-shaped at Mg/Ca molar ratio of 8, not peanut-shaped any longer. The surface of the rod-shaped precipitate was covered by many flaky minerals with a uniform thickness, not nano-scale granular minerals, significantly different from that shown in Figure 5a. Single bacterium in the concave hole of some irregular mineral precipitates could also been observed, and other bacteria were mixed together with the irregular mineral precipitates. The result confirmed that *B. licheniformis* SRB2 bacteria had an effect on the precipitation of the irregular minerals. There are a large number of columnar minerals at Mg/Ca molar ratio of 10 (Figure 5d), besides of the irregular precipitates covered with numerous flaky minerals, indicating that proper Mg/Ca molar ratio and *B. licheniformis* SRB2 bacteria together played an important role in the crystallization of the columnar crystals. Some *B. licheniformis* SRB2 bacteria are living in the concave holes of the columnar minerals, indicating that there was a close relationship between *B. licheniformis* SRB2 bacteria and the columnar crystals. There are also a mass of columnar crystals besides of the irregular precipitates (Figure 5e) at Mg/Ca molar ratio of 12. The length and width of the rhabdoid pit on the surface of the columnar crystals was substantially consistent with the size of a *B. licheniformis* SRB2 bacterium. There is a *B. licheniformis* SRB2 bacterium lying in the pit, indicating there was a close relationship between *B. licheniformis* SRB2 bacterium and the short rhabdoid pit. A small crystal embedded in the large crystal can also be observed. The columnar crystals with inlaying structure did not appear at other Mg/Ca molar ratios. There are no cracks in the columnar minerals, indicating the columnar minerals had a better crystal structure at Mg/Ca molar ratio of 12 than Mg/Ca molar ratio of 10.

Figure 6a shows that the spherical and dumbbell-shaped mineral precipitates in Figure 5a mainly contain C, O and Ca three elements, indicating that the minerals were $CaCO_3$. The minerals also contain a small amount of Na and Si elements. Na element came from the medium. Si element came from the stub supporting the samples, which consists of monocrystalline silicon. Figure 6b shows that it mainly contains C, O and Ca elements, only a small amount of Si element. This result confirmed that the peanut-shaped mineral at Mg/Ca molar ratio of 6 was also $CaCO_3$. Figure 6c and d also show that the rod-shaped precipitates

Preprints (www.preprints.org) | NOT PEER-REVIEWED | Posted: 22 January 2017 doi:10.20944/preprints201701.0096.v1

formed by flaky minerals and the irregular minerals in Figure 5d were also $CaCO_3$. Mg element came from the culture medium, absorbed tightly by the irregular minerals. The columnar mineral in Figure 5d mainly contains C, O and Mg elements, only a small amount of Ca and Si element (Figure 6e). This result confirmed that the columnar minerals were $MgCO_3$. Ca element came from the culture medium. EDX analyses of the irregular mineral and the columnar mineral in Figure 5e shows that it was $CaCO_3$ (Figure 6f) and $MgCO_3$ (Figure 6g) respectively.

B. licheniformis SRB2 bacteria played an important role in the precipitation of carbonates *in vitro*, which could be also proved by the lower concentration of Ca^{2+} and Mg^{2+} in the experimental group than that in the control group at each of Mg/Ca molar ratio. The existence of Mg^{2+} could protect *B. licheniformis* SRB2 bacteria from being encased by the calcite shell, and thus the active *B. licheniformis* SRB2 bacteria could play a normal role in the precipitation of Ca^{2+} and Mg^{2+}. What was more, the application of *B. licheniformis* SRB2 bacteria in hard water could decrease the inhibition effect of Mg^{2+} on calcite precipitation. *B. licheniformis* SRB2 bacteria had an excellent capability to precipitate Ca^{2+} and Mg^{2+} ions, harmless to people and the environment at the same time. Therefore, there was a good prospect for water softening by applying *B. licheniformis* SRB2 bacteria to precipitate Ca^{2+} and Mg^{2+} ions. Although the methods of water softening have constantly been improved in recent years, it has been rarely reported that the microorganism, especially the probiotics beneficial to human health, was applied to water softening.

HRTEM analysis of mineral precipitates at different Mg/Ca molar ratios

The crystal indice (*hkl*) (0114), (217), (128) and (0012) correlates with the calculated interplanar spacing (d, Å) 1.1711, 1.3502, 1.2938 and 1.4258, respectively (Figure 7a), indicating that the mineral precipitate was calcite (PDF#24-0027). The crystal indice (*hkl*) (104), (103) and (101) correlates with the calculated interplanar spacing 3.5036, 4.1162 and 5.8041, respectively (Figure 7b), indicating that it was vaterite (PDF#72-1616). Therefore, the mineral precipitates at Mg/Ca molar ratio of 0 were calcite and vaterite, consistent with the result of EDS analysis shown in Figure 6a. The crystal indice (*hkl*) (221), (103), (220) and (022) correlates with the calculated interplanar spacing 2.4859, 2.4220, 2.6457 and 2.9145, respectively

Preprints (www.preprints.org) | NOT PEER-REVIEWED | Posted: 22 January 2017 doi:10.20944/preprints201701.0096.v1

(Figure 7c), indicating that the mineral precipitates were monohydrocalcite (PDF#83-1923). Monohydrocalcite was composed of Ca, C, O and H element. H element could not be shown by EDS analysis. Thus, the result of HRTEM was consistent with that of EDS analysis in Figure 6b. Figure 7d shows the mineral precipitates were also monohydrocalcite (PDF#83-1923), whose elemental composition was also consistent with EDS result in Figure 6c. Figure 7e shows that the crystal indices (*hkl*) (206), (-222), (-214) and (204) are obtained, and the calculated interplanar spacings (Å) are 1.7836, 2.0819, 2.1836 and 2.3737, respectively. From these HRTEM results, we concluded that the mineral precipitates were nesquehonite (PDF#70-1433). Figure 7f shows that the crystal indices (*hkl*) (012), (201) and (101) are obtained, and the calculated interplanar spacings (Å) are 3.4899, 3.9162 and 5.8203, respectively. From these SAED results, we concluded that the mineral precipitates were monohydrocalcite (PDF#83-1923). Thus, it could be concluded from the above results that the mineral precipitates at Mg/Ca molar ratio of 10 were nesquehonite and monohydrocalcite. Monohydrocalcite was composed of Ca, C, O and H element. Thus, the result of HRTEM was consistent with that of EDS analysis in Figure 6d. Nesquehonite was composed of Mg, C and O element. Thus, the result of SAED was consistent with that of EDS analysis in Figure 6e. It can be seen from Figure 7g and h that the crystals were also nesquehonite (PDF#70-1433) and monohydrocalcite (PDF#83-1923), also consistent with those of EDS analysis (Figure 6f and g).

XRD analysis of the mineral precipitates at different Mg/Ca molar ratios

It can be seen from Figure 8a that the mineral precipitates are calcite in the control group at Mg/Ca molar ratio of 0. The crystal plane (018) of calcite shows a phenomenon of preferential orientation. The diffraction peak intensity of crystal plane (116) should be stronger than that of crystal plane (018) to the standard calcite. However, the opposite is true, and the diffraction peak intensity of crystal plane (018) is stronger than that of crystal plane (116). Figure 8b shows that the mineral precipitates are calcite and vaterite in the experimental group at Mg/Ca molar ratio of 0, which were well consistent with the results of HRTEM and SAED in Figure 7a and b. Calcite had no phenomenon of preferential orientation in the experimental group.

In this study, calcite and vaterite were precipitated in the experimental group and while only calcite was

precipitated in the control group at Mg/Ca molar ratio of 0. The unit cell of calcite was a rhombohedron and vaterite belonged to the hexagonal crystal system [39]. Vaterite is a kind of most unstable anhydrous calcium carbonate, which can be easily transformed into the most stable calcite at ambient temperature and pressure [40]. But when organic factor takes part in the formation process of vaterite, the stability will increase [41]. According to the above conclusion, we could infer vaterite became more stable due to the existence of the organic factor *B. licheniformis* SRB2 bacteria in the experimental group. The surface of cell and exterior structure of bacterium can influence the final result of the mineralization process [42]. *B. licheniformis* SRB2 bacterium was gram-positive, the cytoderm of which was composed of peptidoglycan and teichoic acid. Peptidoglycan was composed of N-acetyglucosamine (G) with alternate N-acetylmuramic (M) through β-(1, 4)-glucosidic bond to form linear glycan chains. M was a lactyl ether group at the C3 position of G, which bound a short-chain peptide composed of four amino acids. The short-chain peptide varied for different strains, including unusual D-glutamic acid, D-alanine, L-diaminopimelic acid and other diamino acids, among of which L-amino acid was arranged with D-amino acid alternately (Figure 9). A number of studies have confirmed that amino acid has an ability to promote the formation of vaterite crystals [43-49]. So in this study, amino acids on peptidoglycan of *B. licheniformis* SRB2 bacteria had a close relationship with the formation of vaterite. The other composition of the cytoderm of gram-positive bacterium was teichoic acid, which was a kind of acidic polysaccharose formed by glycerin residues or ribitol linked together through phosphodiester bond. It has been reported that polysaccharide located in the glycoprotein can increase the stability of vaterite [41]. Maybe teichoic acid located in the cytoderm of *B. licheniformis* SRB2 bacteria had also played the same role as mentioned above. It was maybe the main reason that there was no vaterite precipitated in the control group without *B. licheniformis* SRB2 bacteria.

The mineral precipitates are monohydrocalcite in the control group at Mg/Ca molar ratio of 6. The phenomenon of preferential orientation occurred at crystal plane (301). The diffraction peak intensity of crystal plane (110) should be higher than that of crystal plane (301) to the standard monohydrocalcite. However, the diffraction peak intensity of crystal plane (301) is stronger than that of crystal plane (110). The mineral precipitates are also monohydrocalcite in the experimental group, well consistent with the result of

Preprints (www.preprints.org) | NOT PEER-REVIEWED | Posted: 22 January 2017 doi:10.20944/preprints201701.0096.v1

HRTEM in Figure 7c. Monohydrocalcite in the experimental group had the same phenomenon of preferential orientation. The mineral precipitates are also monohydrocalcite in the control group at Mg/Ca molar ratio of 8. The phenomenon of preferential orientation not only occurred at crystal faces (301), but also occurred at crystal faces (11-2). The diffraction peak intensity of crystal plane (11-1) should be higher than that of crystal plane (11-2) to the standard monohydrocalcite. However, the diffraction peak intensity of crystal plane (11-2) is higher than that of crystal plane (11-1). The mineral precipitates in the experimental group are also monohydrocalcite, well consistent with the result of HRTEM in Figure 7d. Monohydrocalcite in the experimental group also had the same phenomena of preferential orientation for crystal faces (301) and (11-2).

The mineral precipitates are also monohydrocalcite in the control group at Mg/Ca molar ratio of 10. The phenomenon of preferential orientation only occurs at crystal faces (301). The mineral precipitates are nesquehonite and monohydrocalcite in the experimental group, well consistent with the results of HRTEM and SAED in Figure 7e and f. Nesquehonite also has a phenomenon of preferential orientation. The diffraction peak intensity of crystal plane (101) should be higher than that of crystal plane (002) to the standard nesquehonite. However, the diffraction peak intensity of crystal plane (002) is higher than that of crystal plane (101). Thus, the phenomenon of preferential orientation of nesquehonite occurred at crystal faces (002). Similarly, the diffraction peak intensity of crystal plane (400) should be higher than that of crystal plane (004) to the standard nesquehonite, however, the diffraction peak intensity of crystal plane (004) is higher than that of crystal plane (400). Thus, the phenomenon of preferential orientation of nesquehonite also occurred to crystal faces (004). The mineral precipitates are also monohydrocalcite in the control group at Mg/Ca molar ratio of 12. The phenomenon of preferential orientation only occurs to crystal faces (301). The mineral precipitates are nesquehonite and monohydrocalcite in the experimental group, well consistent with the results of HRTEM and SAED in Figure 7g and h. The phenomena of preferential orientation of nesquehonite not only occurred to crystal faces (002), but also crystal faces (004).

This experiment confirmed that *B. licheniformis* SRB2 bacteria could induce the precipitation of a large number of nesquehonite crystals and a small quantity of monohydrocalcite crystals in the experimental

group at Mg/Ca molar ratio of 10 and 12, but there was only monohydrocalcite without nesquehonite precipitated in the control group at the same Mg/Ca molar ratio. Therefore, the nucleation and growth of nesquehonite crystal was due to the existence of *B. licheniformis* SRB2 bacteria, which could increase the pH value of the culture medium from 7.6 to 8.4. Ammonia generated through the metabolism of heterotrophic bacteria in the culture medium would lead to the formation of excess hydroxyl [50], which was maybe the main reason for the increase of pH value in the experimental group. The increase of pH value was prerequisite for carbonate precipitation [51]. Microorganisms often promote the formation of highly supersaturated microenvironments to facilitate the precipitation of carbonates, e.g., bacterial cells can absorb Ca, Mg or other metallic cations and act as nucleation sites, even when the supersaturation has not been reached in the surrounding environment [52]. In the nesquehonite formation process, the concentration of Mg^{2+} was likely to be very important. Mg needs higher energy to dehydrate before incorporating into a carbonate structure or controlling the crystal growth due to the stronger hydration shell of Mg in comparison to Ca [53]. Under the action of *B. licheniformis* SRB2 bacteria, the kinetic inhibitor could be removed and a high concentration of free available Mg^{2+} would tend to combine with the bicarbonate ions and hydroxyl ions to promote the precipitation of nesquehonite crystals. Based on the results of our culture experiments, we proposed that the presence of specific *B. licheniformis* SRB2 bacteria could mediate nesquehonite precipitation and overcome the kinetic barriers. Nesquehonite was precipitated only at Mg/Ca molar ratio of 10 and 12, not at Mg/Ca molar ratio of 0, 6 and 8 in the experimental group, indicating that enough high Mg/Ca molar ratio was the other factor for nesquehonite precipitation.

The diffraction peak intensities of mineral precipitates in the control group are far below than those in the experimental group (Figure 8), indicating that the mineral precipitates in the experimental group had a better crystal structure. The only difference between the experimental group and the control group was the presence of *B. licheniformis* SRB2 bacteria. Thus, the formation of new minerals with better crystal structure had a close relationship with the existence of biological factor *B. licheniformis* SRB2 bacteria.

Preprints (www.preprints.org) | NOT PEER-REVIEWED | Posted: 22 January 2017 doi:10.20944/preprints201701.0096.v1

The role of *Bacillus licheniformis* SRB2 in the carbonates precipitation

Bacteria are the key organisms in the formation of the microbial carbonates minerals [54]. On the one hand, the extracellular polymeric substance (EPS) of bacteria could absorb positive ions (Ca^{2+}, Mg^{2+}) due to its electronegativity. Not only that, minerals can also nucleate both inside and outside the cell wall of microorganism [55]. In addition that, the life activities of bacteria are also key factors that influenced the formation of minerals, such as the photosynthesis of cyanobacteria, and the redox processes of anaerobic heterotrophs [54, 55].

In present study, the primary impact on biomineralization of *Bacillus licheniformis* SRB2 was regarded was the function of urease enzyme and nucleation sites on EPS. *Bacillus licheniformis* SRB2 could produce urease enzyme that catalyzed the hydrolysis of urea to produce carbamate and ammonia, and the pH of the culture medium was increased. Even though there was no urea in the culture medium, the metabolism of tryptone could also produce a lot of urea for further use. Many biochemical reactions occurring could lead to the formation of calcium carbonate as shown in Eqs.

$$CO(NH_2)_2 + H_2O \rightarrow NH_2COOH + NH_3 \uparrow$$

As a result, 1 mol of carbonic acid and ammonia are formed because of hydrolyses of carbamate.

$$NH_2COOH + H_2O \rightarrow NH_3 + H_2CO_3$$

After that, these products subsequently form 1 mole of bicarbonate and 2 moles of ammonium and hydroxide ions respectively.

$$H_2CO_3 \rightarrow H^+ + HCO_3^-$$

$$2NH_3 + 2H_2O \rightarrow 2NH_4^+ + 2OH^-$$

In this series of reactions, the pH and the concentration of CO_3^{2-} of culture medium were increased

Preprints (www.preprints.org) | NOT PEER-REVIEWED | Posted: 22 January 2017 doi:10.20944/preprints201701.0096.v1

consequently, and leading to the precipitation of carbonate minerals.

$$HCO_3^- + H^+ + 2NH_4^+ + 2OH^- \rightarrow CO_3^{2-} + 2NH_4^+ + 2H_2O$$

Not only that, the EPS and the bacteria itself provided numerous nucleation sites. Positive ions were absorbed on them and continued to grow as shown in Eqs.

$$EPS + Ca^{2+} / Mg^{2+} \rightarrow EPS \cdot Ca^{2+} \cdot Mg^{2+}$$

$$Cell + Ca^{2+} / Mg^{2+} \rightarrow Cell \cdot Ca^{2+} \cdot Mg^{2+}$$

Finally, it was deposited in the bottom of culture medium as shown in Eqs.

$$EPS \cdot Ca^{2+} \cdot Mg^{2+} + CO_3^{2-} \rightarrow Carbonates \downarrow$$

$$Cell \cdot Ca^{2+} \cdot Mg^{2+} + CO_3^{2-} \rightarrow Carbonates \downarrow$$

4. Conclusions

In present experiments, we have demonstrated that a newly isolated bacterial strain *B. licheniformis* SRB2 are capable of mediating the biomineralization of nesquehonite and monohydrocalcite minerals in a synthetic aerobic medium with 3% NaCl and different Mg/Ca molar ratios. Only monohydrocalcite and calcite mineral crystals could be precipitated in absence of *B. licheniformis* SRB2 bacteria. The bio-precipitation of nesquehonite showed a phenomenon of preferred orientation. The concentration of Ca^{2+} and Mg^{2+} in the experimental group was much lower than that in the control group at different Mg/Ca molar ratios because of the effect of bacteria. Therefore, the above result suggested that *B. licheniformis* SRB2 bacteria could be used to precipitate Mg^{2+} and Ca^{2+} ions from hard water through biomineralization of Ca^{2+} and Mg^{2+}. *B. licheniformis* SRB2 bacteria had a capability to reduce the inhibition effect of Mg^{2+} on the precipitation of Ca^{2+}. The quantity of Ca^{2+} ions used to precipitate carbonate calcium increased due to the metabolic activity of *B. licheniformis* SRB2 bacteria. In conclusion, this experimental study could give new

insights into bio-precipitation of carbonate minerals and water softening mediated by microbes. Applying probiotics to precipitate Mg^{2+} and Ca^{2+} ions in water softening will have potential application value.

Acknowledgements

This work was supported by the National Natural Science Foundation of China (41372108, U1663201), Open Fund of the Key Laboratory of Marine Geology and Environment, Chinese Academy of Sciences (No. MGE2016KG10), the Specialized Research Fund for the Doctoral Program of Higher Education (20133718130001), and supported by SDUST Research Fund (2015TDJH101), Shandong Provincial Key Laboratory of Depositional Mineralization and Sedimentary Minerals (DMSM201412), Shandong Province Natural Science Foundation (ZR2014DM005), the China Postdoctoral Science Foundation Funded Project (2016M600548), Qingdao Postdoctoral Applied Research Project (2015199).

References

1. Cao, XX.; Huang, X.; Liang, P.; Xiao, K.; Zhou, YJ.; Zhang, XY.; Logan BE. A new method for water desalination using microbial desalination cells. *Environ. Sci. Technol.* **2009**, 43, 7148-7152.
2. Zhang, B.; He, Z. Integrated salinity reduction and water recovery in an osmotic microbial desalination cell. *Rsc. Advances.* **2012**, 2, 3265-3269.
3. Shannon, MA.; Bohn, PW.; Elimelech, M.; Georgiadis, JG.; Mariñas, BJ.; Mayes, AM. Science and technology for water purification in the coming decades. *Nature.* **2008**, 452, 301-310.
4. Khawaji, AD.; Kutubkhanah, IK.; Wie, JM. Advances in seawater desalination technologies. *Desalination.* **2008**, 221, 47-69.
5. Charcosset, C. A review of membrane processes and renewable energies for desalination. *Desalination*. **2009**, 245, 214-231.
6. Pendergast, MTM.; Hoek, EMV. A review of water treatment membrane nanotechnologies. *Energ. Environ. Sci.* **2011**, 4, 1946-1971.
7. Mohsenzadeh, F.; Rad, AC.; Akbari, M. Evaluation of oil removal efficiency and enzymatic activity in some fungal strains for bioremediation of petroleum-polluted soils. *Iran. J. Environ. Health. Sci. Eng.*

2012, 9, 1–8.

8. Choudhary, S.; Sar, P. Uranium biomineralization by a metal resistant *Pseudomonas aeruginosa* strain isolated from contaminated mine waste. *J. Hazard. Mater.* **2011**, 186, 336-343.
9. Achal, V.; Pan, XL.; Fu, QL.; Zhang, DY. Biomineralization based remediation of As (III) contaminated soil by *Sporosarcina ginsengisoli*. *J. Hazard. Mater.* **2015**, 201, 178-184.
10. Ginisty, P.; Guezennec, J. Biosorption of cobalt by *Pseudomonas halodenitrificans*: influence of cell wall treatment by alkali and alkaline earth metals and ionexchange mechanisms. *Biotechnol. Lett.* **1998**, 20, 1035-1039.
11. Da, Costa AA.; De Franca, FP. Cadmium uptake by *Spirulina maxima*: toxicity and mechanism. *World. J. Microb. Biot.* **1998**, 14, 579-581.
12. Riordan, C.; Bustard, M.; Putt; R. Removal of uranium from solution using residual brewery yeast: combined biosorption and precipitation. *Biotechnol. Lett.* **1997**, 19, 385-387.
13. Szilva, J.; Kuncová, G.; Patzák, M.; Dostálek, P. The application of a sol-gel technique to preparation of a heavy metal biosorbent from yeast cells. *J. Sol-Gel. Sci. Techn.* **1998**, 13, 289-294.
14. Gomes, NCM.; Figueira, MM.; Camargos, ERS.; Mendonça-Hagler, LCS.; Dias, JCT.; Linardi, VR. Cyano-metal complexes uptake by *Aspergillus niger*. *Biotechnol. Lett*. **1999**, 21, 487-490.
15. Bhainsa KC,; D'Souza, SF. Biosorption of uranium (VI) by *Aspergillus fumigatus*. *Biotechnol. Tech.* **1999**, 13, 695-699.
16. Zhang, XZ.; Luo, SG.; Yang, Q.; Zhang, HL.; JY, Li.; Accumulation of uraniumat low concentration by the green alga *Scenedesmus obliquus* 34. *J. Appl. Phycol.* **1997**, 9, 65-71.
17. Omar, HH. Adsorption of zinc ions by *Scenedesmus obliquus* and *S. quadricauda* and its effect on growth and metabolism. *Biol. Plantarum.* **2002**, 45, 261-266.
18. Matheickal, JT.; Yu, Q. Cu(II) binding by marine alga *Ecklonia radita* biomaterial. *Env. Tech.* **1997**, 18, 25-34.
19. Ligy, P.; Leela, I.; Venkobachar, C. Site of interaction of copperon bacillus polymyxa. *Water. Air. Soil. Poll.* **2000**, 119, 11-21.

20. Chen, Z.; Pan, XH.; Chen, H.; Guan, X.; Lin, Z. Biomineralization of Pb (II) into Pb-hydroxyapatite induced by *Bacillus cereus* 12-2 isolated from Lead-Zinc mine tailings. *J. Hazard. Mater.* **2016**, 301, 531-537.

21. Jafari, M.; Shafaei, S Z A.; Abdollahi, H.; et al. A Comparative Study on the Effect of Flotation Reagents on Growth and Iron Oxidation Activities of Leptospirillum ferrooxidans and Acidithiobacillus ferrooxidans. *Minerals*, **2016**, 7, 2.

22. Govarthanan. M.; Lee. KJ.; Cho, M.; Kimb, JS.; Kamala-Kannana, S.; Oh, BT. Significance of autochthonous *Bacillus sp.* KK1 on biomineralization of lead in mine tailings. *Chemosphere.* **2013**, 90, 2267-2272.

23. Lian, B.; Hu, QN.; Chen, J.; Ji, JF.; Teng, HH. Carbonate biomineralization induced by soil bacterium *Bacillus megaterium*. Geochim. Cosmochim. Ac. **2006**, 70, 5522-5535.

24. Pan, XH.; Chen, Z.; Chen, FB.; Cheng, YJ.; Lin, Z.; Guan, X. The mechanism of uranium transformation from U (VI) into nano-uramphite by two indigenous *Bacillus thuringiensis* strains. *J. Hazard. Mater.* **2015**, 297, 313-319.

25. Han, ZZ.; Zhao, YY.; Yan, HX.; Zhao, H.; Han, M.; Sun, B.; Sun, XY.; Hou, FF.; Sun, H.; Hao, L.; Sun, YB.; Wang, J.; Li, H.; Wang, YQ.; Du, H. Struvite Precipitation Induced by a Novel Sulfate-Reducing Bacterium *Acinetobacter* calcoaceticus SRB4 Isolated from River Sediment. *Geomicrobiology*. **2015**, 32, 868-877.

26. Li, X.; Gou, XY.; Long, D.; Ji, ZX.; Hu, LF.; Xu, DH.; Liu, J.; Chen, SW. Physiological and metabolic analysis of nitrate reduction on poly-gamma-glutamic acid synthesis in *Bacillus* licheniformis WX-02. *Arch. Microbiol.* **2014**, 196: 791-799.

27. Reddy, MM.; Nancollas, GH. The crystallization of calcium carbonate IV. The effect of magnesium, strontium and sulfate ions. *J. Cryst.* Growth. **1976**, 35, 33-38.

28. Akin, GW.; Lagerwerff, JV. Calcium carbonate equilibria in aqueous solutions open to the air. I. The solubility of calcite in relation to ionic strength. *Geochim. Cosmochim. Ac.* **1965**, 29, 343-352.

29. House, WA.; Howson, MR. Crystallisation kinetics of calcite in the presence of magnesium ions. *J Chem*

Soc, Faraday. Trans. **1988**, 184, 2723-2734.

30. Paquette, J.; Reeder, RJ. Relationship between surface structure, growth mechanism and trace element incorporation in calcite. *Geochim. Cosmochim. Ac.* **1995**, 59, 735-749.
31. Dawe. AR.; Zhang, Y. Kinetics of calcium carbonate scaling using observations from glass micromodels. *J. Petrol. Sci. Eng.* **1997**, 18, 179-187.
32. Zhang, Y.; Dawe, RA. Influence of Mg^{2+} on the kinetics of calcite precipitation and calcite crystal morphology. *Chem. Geol.* **2000**, 163, 129-138.
33. Wright, DT.; Oren, A. Nonphotosynthetic bacteria and the formation of carbonates and evaporites through time. *Geomicrobiol. J.* **2005**, 22: 27-53.
34. Dupraz, C.; Visscher, PT. Microbial lithification in marine stromatolites and hypersaline mats. *Trends. Microbiol.* **2005**, 13, 429-438.
35. Riding, R. Microbial carbonates: the geological record of calcified bacterial-algal mats and biofilms. *Sedimentology.* **2002**, 47, 179-214.
36. Stocks-Fischer, S.; Galinat, JK.; Bang, S. Microbiological precipitation of $CaCO_3$. *Soil. Biol. Biochem.* **1999**, 31, 1563-1571.
37. Tourney, J.; Ngwenya, BT. Bacterial extracellular polymeric substances (EPS) mediate $CaCO_3$ morphology and polymorphism. *Chem. Geol.* **2009**, 262, 138-146.
38. Berner, RA. The role of magnesium in the crystal growth of calcite and aragonite from sea water. *Geochim. Cosmochim. Ac.* **1975**, 39, 489- 494.
39. Sommerdijk, NAJ.; de With G. Biomimetic $CaCO_3$ mineralization using designer molecules and interfaces. *Chem. Rev.* **2008**, 108, 4499-4550.
40. Suzuki, M.; Nagasawa, H.; Kogure, T. Synthesis and structure of hollow calcite particles. *Cryst. Growth. Des.* **2006**, 6, 2004-2006.
41. Daskalakis, MI.; Magoulas, A.; Kotoulas, G.; Katsikis, I.; Bakolas, A.; Karageorgis, AP.; Mavridou, A.; Doulia, D.; Rigas, F. Cupriavidus metallidurans biomineralization ability and its application as a bioconsolidation enhancer for ornamental marble stone. *Appl. Microbiol. Biot.* **2014**, 98, 6871-6883.

 doi:10.20944/preprints201701.0096.v1

42. De, Muynck, W.; De, Belie, N.; Verstraete, W. Microbial carbonate precipitation in construction materials: a review. *Ecol. Eng.* **2010**, 36, 118-136.

43. Manoli, F.; Dalas, E. Calcium carbonate crystallization in the presence of glutamic acid. *J. Cryst. Growth.* **2001**, 222, 293-297.

44. Malkaj, P.; Kanakis, J.; Dalas, E. The effect of leucine on the crystal growth of calcium carbonate. *J. Cryst. Growth.* **2004**, 266, 533-538.

45. Malkaj, P.; Dalas, E. Calcium carbonate crystallization in the presence of aspartic acid. *Cryst. Growth. Des.* **2004**, 4, 721-723.

46. Xie, AJ.; Shen, YH.; Zhang, CY.; Yuan, ZW.; Zhu, XM.; Yang, YM. Crystal growth of calcium carbonate with various morphologies in different amino acid systems. *J. Cryst. Growth.* **2005**, 285, 436-443.

47. Shivkumara, C.; Singh, P.; Gupta, A.; Hedge, MS. Synthesis of vaterite $CaCO_3$ by direct precipitation using glycine and L-alanine as directing agents. *Mater. Res. Bull.* **2006**, 41, 1455-1460.

48. Tong, H.; Ma, W.; Wang, L.; Wan, P.; Hu, J.; Cao, L. Control over the crystal phase, shape, size and aggregation of the calcium carbonate via a L-aspartic acid inducing process. *Biomaterials.* **2004**, 25, 3923-3929.

49. Wolf, SE.; Loges, N.; Mathiasch, B.; Panthöfer, M.; Mey, I.; Janshoff, A.; Wolfgang, T. Phase selection of calcium carbonate through the chirality of adsorbed amino acids. *Angew. Chem. Int. Ed.* **2007**, 46, 5618-5623.

50. Nothdurft, LD.; Webb, GE.; Buster, NA.; Holmes, CW.; Sorauf, JE.; Kloprogge, JT. Brucite microbialites in living coral skeletons: Indicators of extreme microenvironments in shallow-marine settings. *Geology*. **2005**, 33, 169-172.

51. Castanier, S.; Métayer-Levrel, GL.; Perthuisot, JP. Ca-carbonates precipitation and limestone genesis—The microbiogeologist point of view. *Sediment. Geol.* **1999**, 126, 9-23.

52. Rodriguez-Blanco, JD.; Shaw, S.; Bots, P.; Roncal-Herrero, T.; Benning, LG. The role of Mg in the crystallization of monohydrocalcite. *Geochim. Cosmochim. Ac.* **2014**, 127, 204-220.

53. Di, Tommaso, D.; De, Leeuw, NH. Structure and dynamics of the hydrated magnesium ion and of the

solvated magnesium carbonates: insights from first principles simulations. *Phys. Chem. Chem. Phys.* **2010**, 12, 894–901.

54. Riding R. Microbial carbonates: the geological record of calcified bacterial–algal mats and biofilms. *Sedimentology*, **2000,** 47(s1): 179-214.

55. Han Z, Zhao Y, Yan H, et al. The Characterization of Intracellular and Extracellular Biomineralization Induced by Synechocystis sp. PCC6803 Cultured under Low Mg/Ca Ratios Conditions. *Geomicrobiology*, **2016**: 1-12.

Figure captions

Figure 1. The morphology of SRB2 bacterium and the phylogenetic tree constructed with a neighbor-joining analysis based on a sequence alignment of bacterial 16S rRNA genes **a** TEM image of SRB2 bacterium, **b** Phylogenetic tree

Figure 2. The growth curves of SRB2 bacteria and pH variation tendency at different NaCl concentrations **a** the growth curves, **b** the pH variation tendency

Figure 3. The changes of Ca^{2+} concentration in **a** the control group, **b** the experimental group

Figure 4. The changes of Mg^{2+} concentration in **a** the control group, **b** the experimental group

Figure 5. FE-SEM images of the mineral precipitates in the experimental group for 12 days of culture at **a** Mg/Ca molar ratio = 0, **b** Mg/Ca molar ratio = 6, **c** Mg/Ca molar ratio = 8, **d** Mg/Ca molar ratio = 10, **e** Mg/Ca molar ratio = 12

Figure 6. EDS images of the mineral precipitates in the experimental group for 12 days of culture at **a** Mg/Ca molar ratio = 0, **b** Mg/Ca molar ratio = 6, **c** Mg/Ca molar ratio = 8, **d and e** Mg/Ca molar ratio = 10, **f and g** Mg/Ca molar ratio = 12

Figure 7. HRTEM and SAED images of the mineral precipitates in the experimental group for 12 days of culture at **a and b** Mg/Ca molar ratio = 0, **c** Mg/Ca molar ratio = 6, **d** Mg/Ca molar ratio = 8, **e and f** Mg/Ca molar ratio = 10, **g and h** Mg/Ca molar ratio = 12

Figure 8. XRD images of the mineral precipitates for 12 days of culture in **a** the control group, **b** the experimental group

Figure 9. Peptidoglycan of cell wall (Gram-positive bacteria)

Preprints (www.preprints.org) | NOT PEER-REVIEWED | Posted: 22 January 2017 doi:10.20944/preprints201701.0096.v1

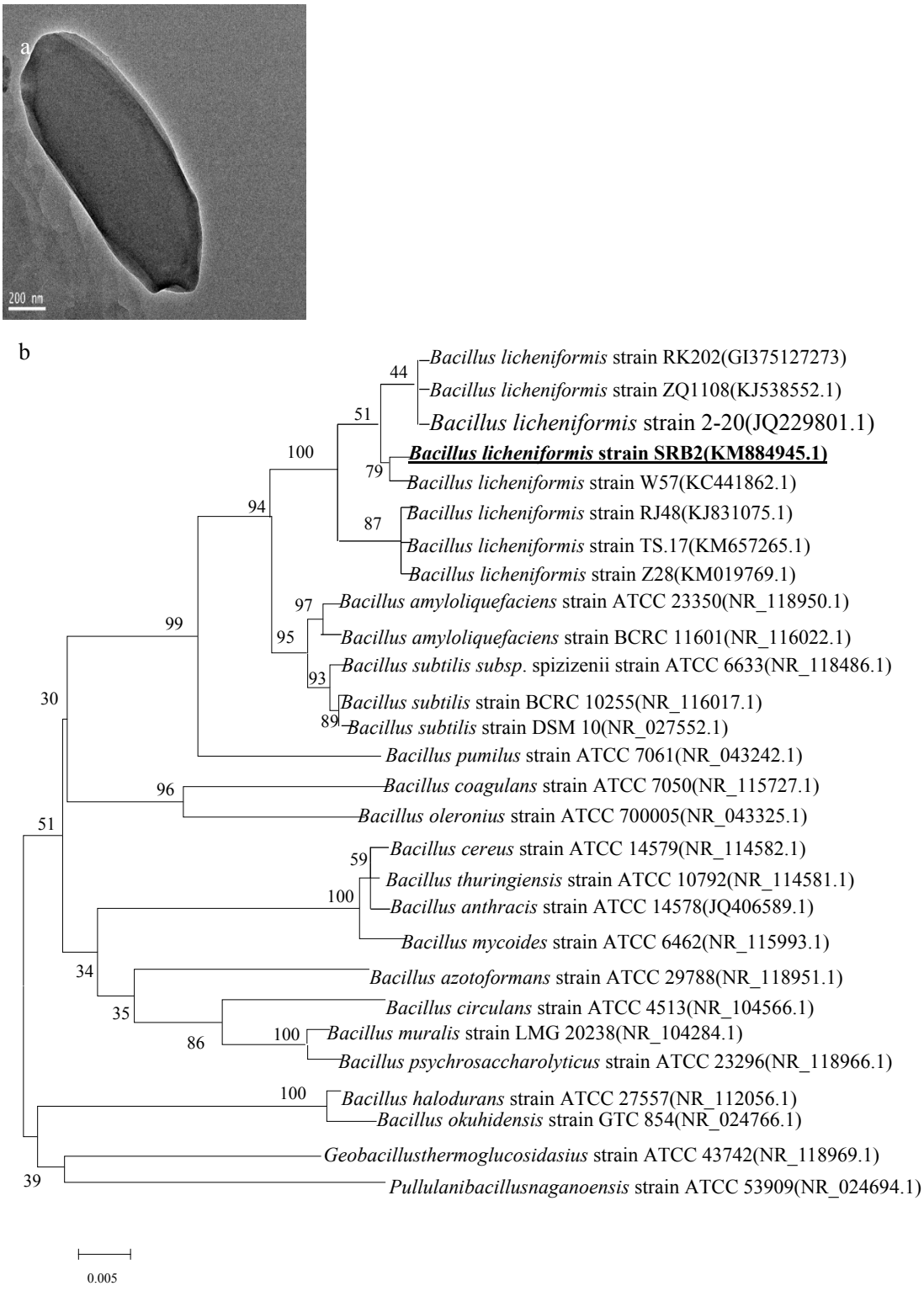

Figure 1. The morphology of SRB2 bacterium and the phylogenetic tree constructed with a neighbor-joining analysis based on a sequence alignment of bacterial 16S rRNA genes **a** TEM image of SRB2 bacterium, **b** Phylogenetic tree

Preprints (www.preprints.org) | NOT PEER-REVIEWED | Posted: 22 January 2017 doi:10.20944/preprints201701.0096.v1

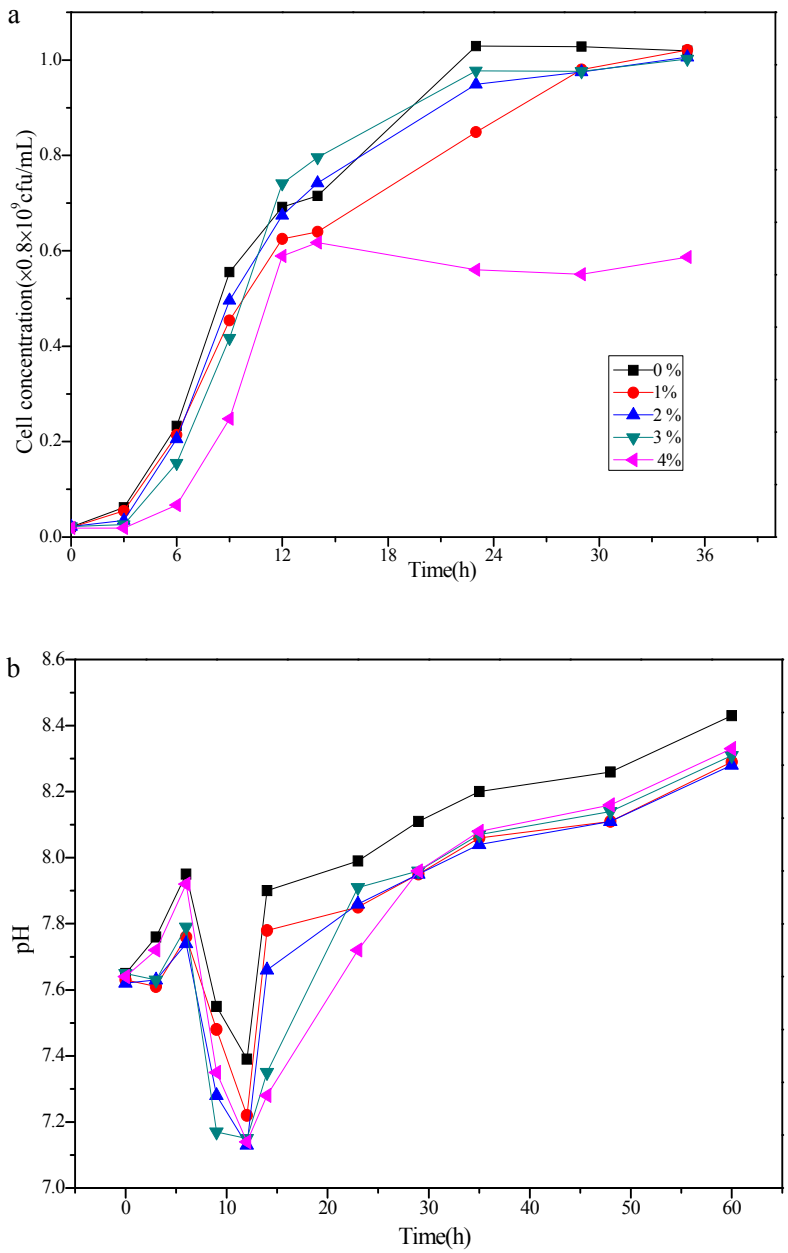

Figure 2. The growth curves of SRB2 bacteria and pH variation tendency at different NaCl concentrations **a** the growth curves, **b** the pH variation tendency

Preprints (www.preprints.org) | NOT PEER-REVIEWED | Posted: 22 January 2017 doi:10.20944/preprints201701.0096.v1

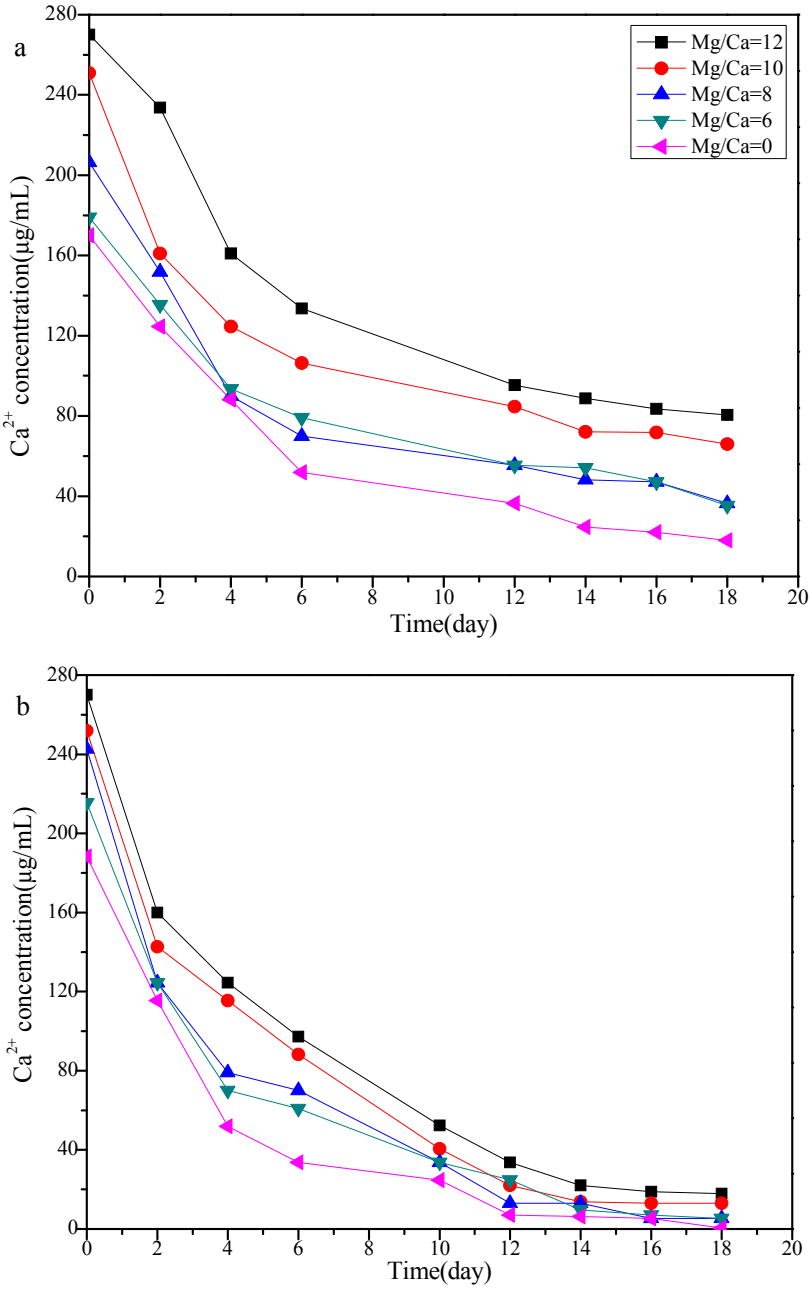

Figure 3. The changes of Ca^{2+} concentration in **a** the control group, **b** the experimental group

Preprints (www.preprints.org) | NOT PEER-REVIEWED | Posted: 22 January 2017 doi:10.20944/preprints201701.0096.v1

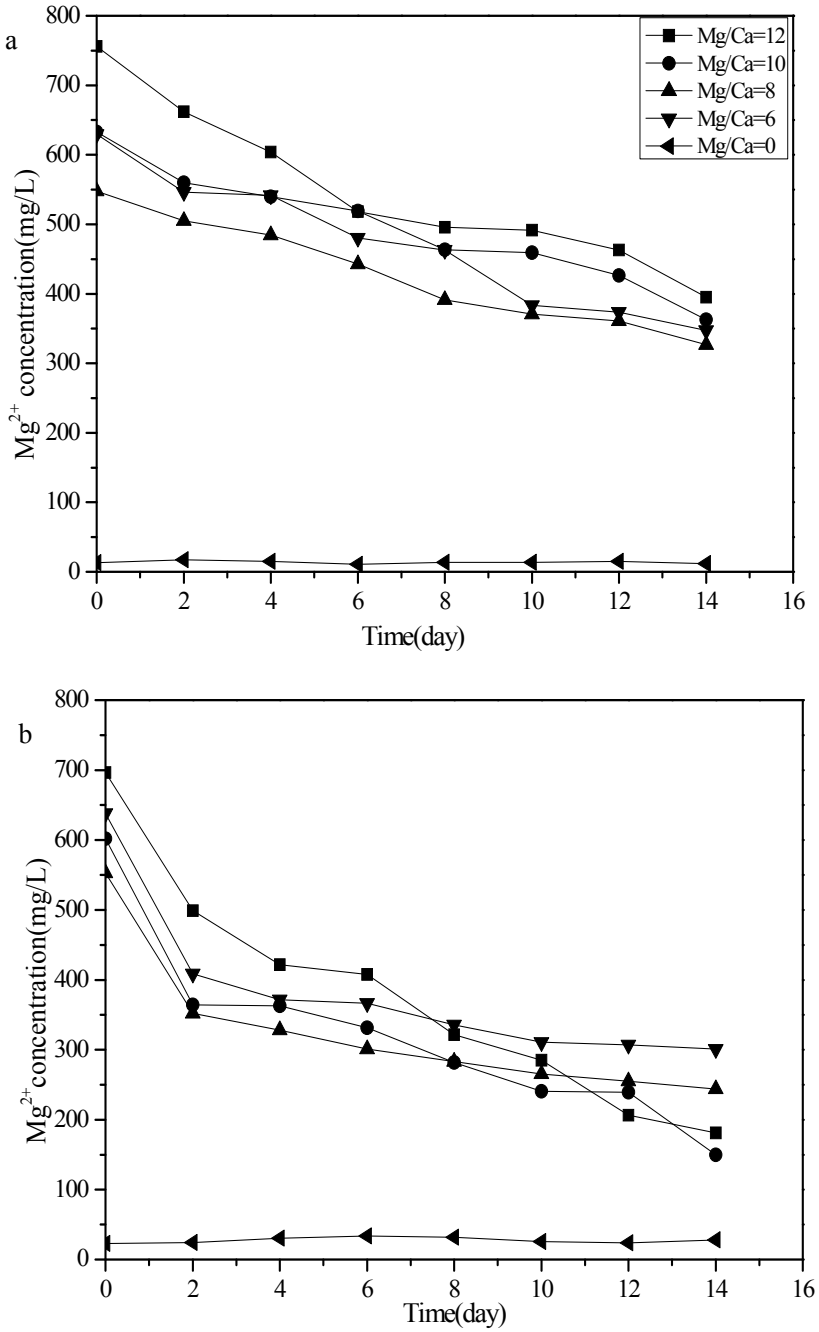

Figure 4. The changes of Mg^{2+} concentration in **a** the control group, **b** the experimental group

Preprints (www.preprints.org) | NOT PEER-REVIEWED | Posted: 22 January 2017 doi:10.20944/preprints201701.0096.v1

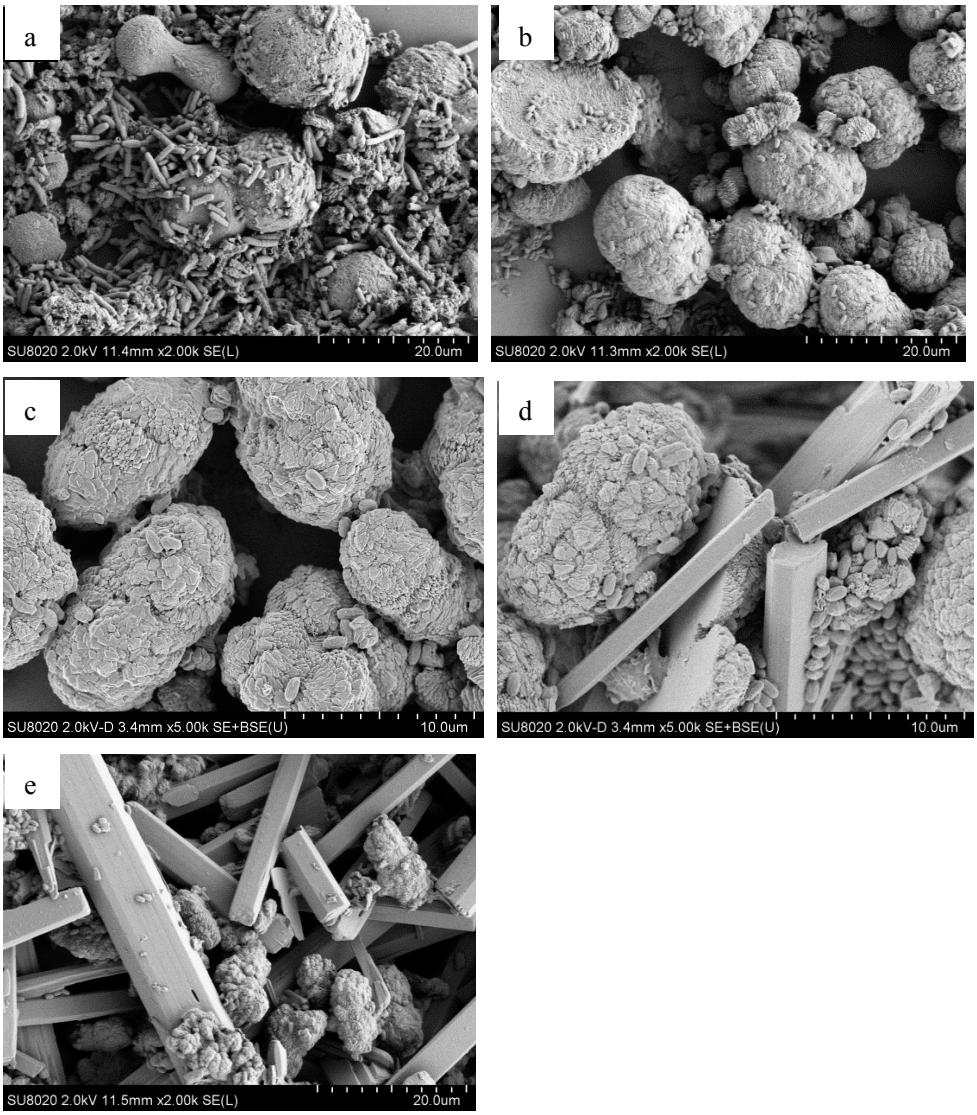

Figure 5. FE-SEM images of the mineral precipitates in the experimental group for 12 days of culture at **a** Mg/Ca molar ratio = 0, **b** Mg/Ca molar ratio = 6, **c** Mg/Ca molar ratio = 8, **d** Mg/Ca molar ratio = 10, **e** Mg/Ca molar ratio = 12

Preprints (www.preprints.org) | NOT PEER-REVIEWED | Posted: 22 January 2017 doi:10.20944/preprints201701.0096.v1

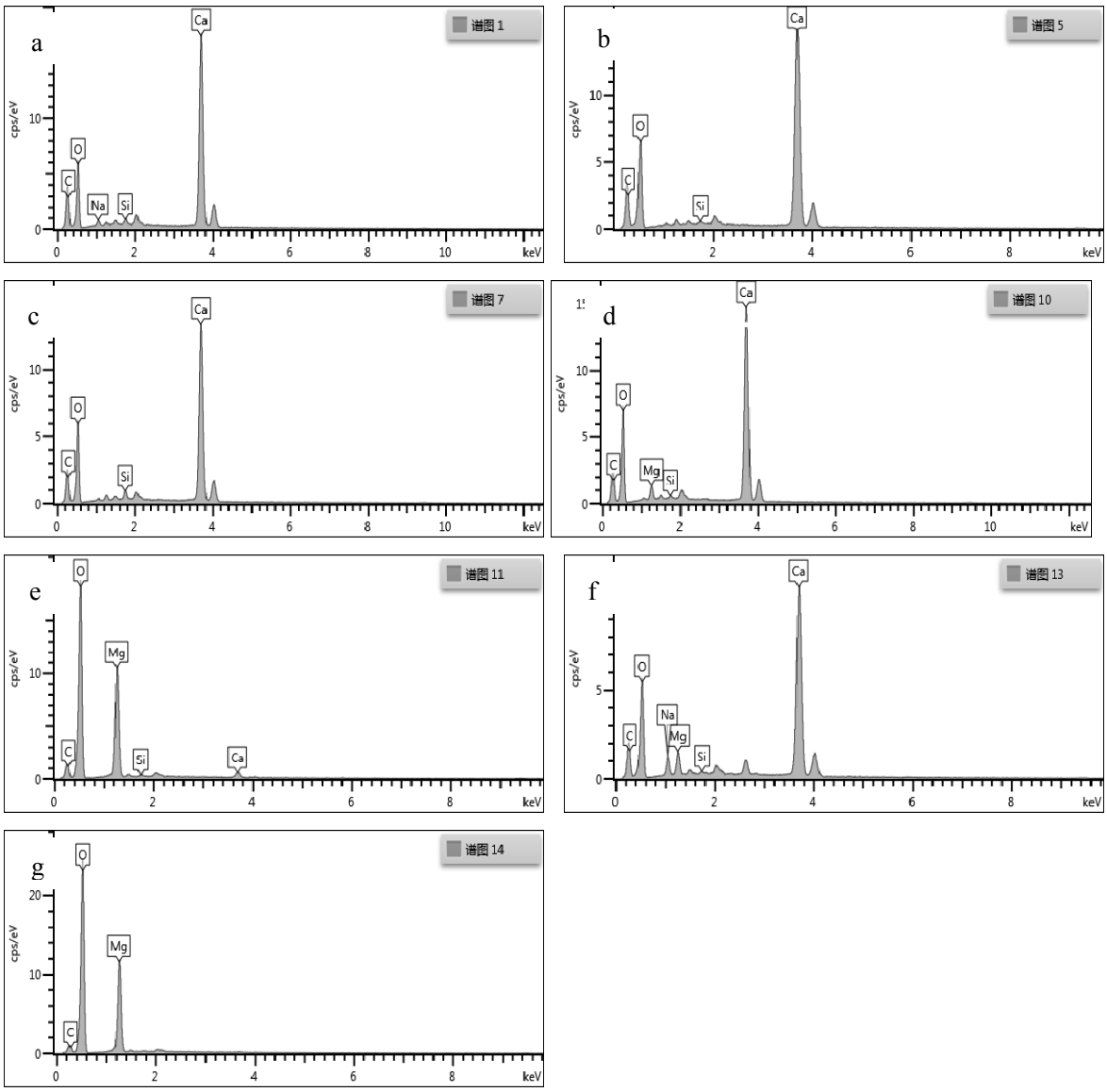

Figure 6. EDS images of the mineral precipitates in the experimental group for 12 days of culture at **a** Mg/Ca molar ratio = 0, **b** Mg/Ca molar ratio = 6, **c** Mg/Ca molar ratio = 8, **d and e** Mg/Ca molar ratio = 10, **f and g** Mg/Ca molar ratio = 12

Preprints (www.preprints.org) | NOT PEER-REVIEWED | Posted: 22 January 2017 doi:10.20944/preprints201701.0096.v1

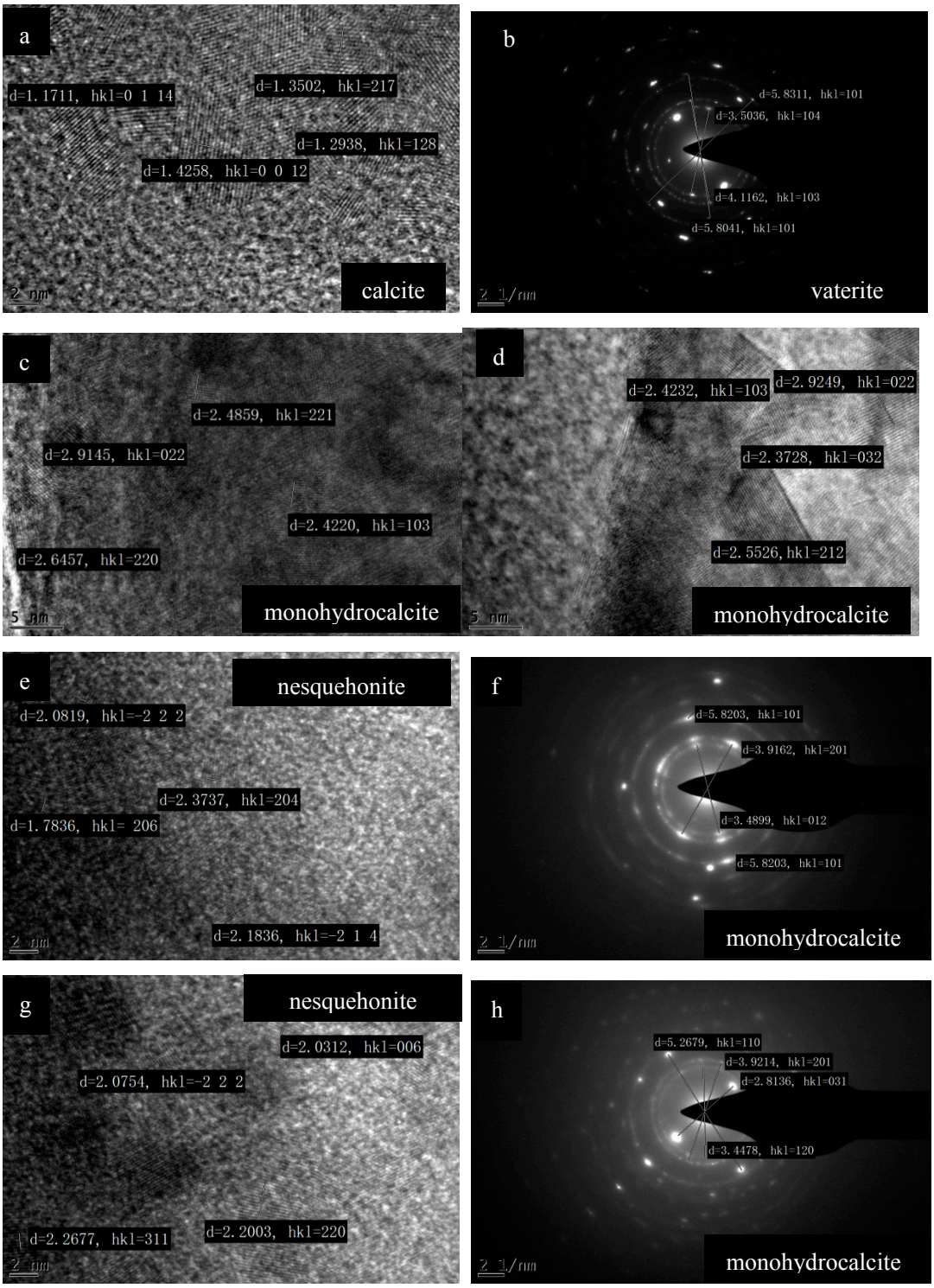

Figure 7. HRTEM and SAED images of the mineral precipitates in the experimental group for 12 days of culture at **a and b** Mg/Ca molar ratio = 0, **c** Mg/Ca molar ratio = 6, **d** Mg/Ca molar ratio = 8, **e and f** Mg/Ca molar ratio = 10, **g and h** Mg/Ca molar ratio = 12

Preprints (www.preprints.org) | NOT PEER-REVIEWED | Posted: 22 January 2017 doi:10.20944/preprints201701.0096.v1

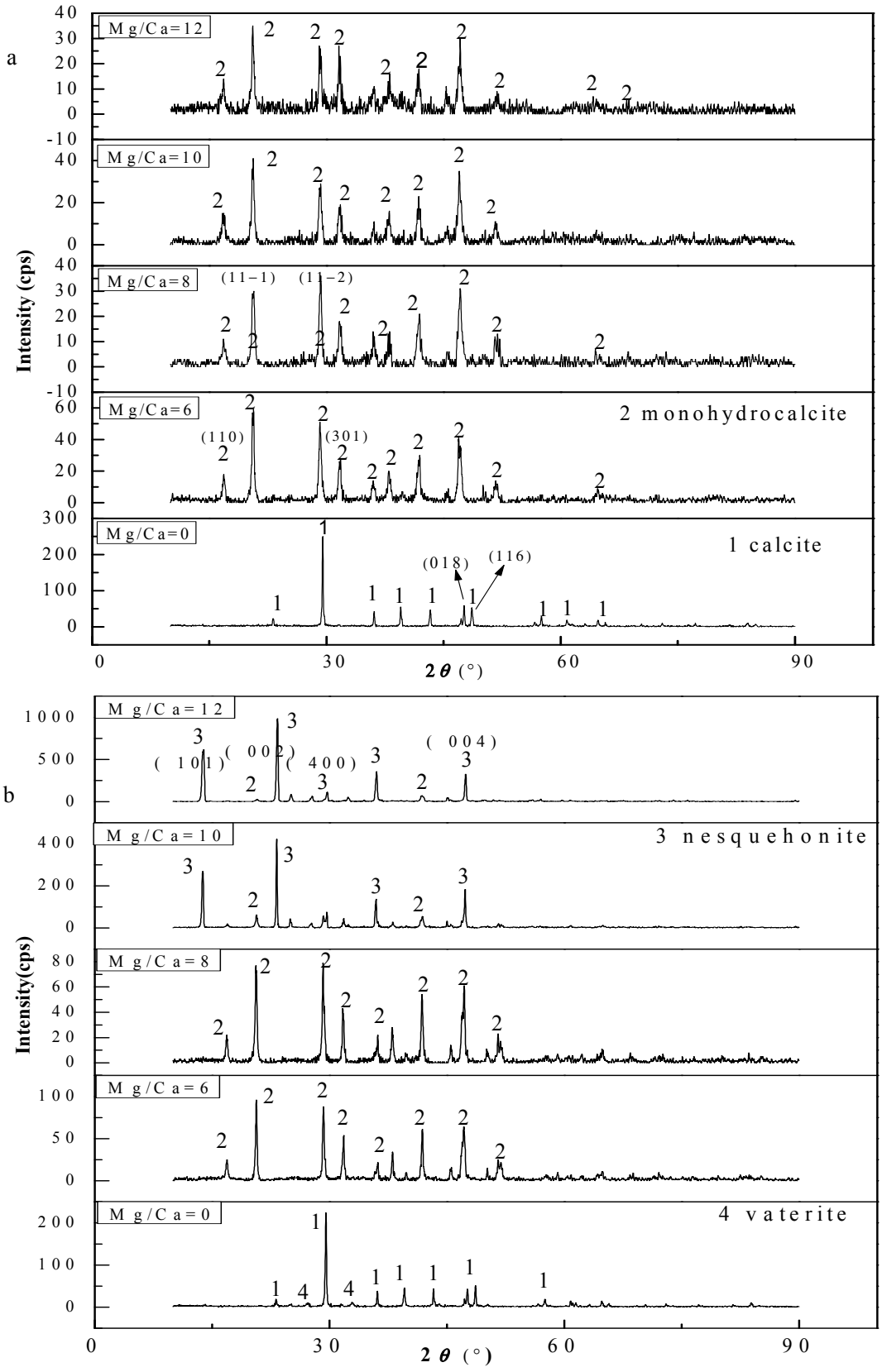

Figure 8. XRD images of the mineral precipitates for 12 days of culture in **a** the control group, **b** the experimental group

Figure 9. Peptidoglycan of cell wall (Gram-positive bacteria)